ACS OMEGA

Open Access

http://pubs.acs.org/journal/acsodf

Article

Two-Phase Crude Oil–Water Flow Through Different Pipes: An Experimental Investigation Coupled with Computational Fluid Dynamics Approach

Shirsendu Banerjee,* Anirban Banik, Vinay Kumar Rajak, Tarun Kanti Bandyopadhyay, Jayato Nayak, Michał Jasinski, Ramesh Kumar, Byong-Hun Jeon,* Masoom Raza Siddiqui, Moonis Ali Khan, Sankha Chakrabortty, and Suraj K. Tripathy*

Cite This: *ACS Omega* 2024, 9, 11181−11193

Read Online

ACCESS | Metrics & More | Article Recommendations | Supporting Information

ABSTRACT: The present study deals with two-phase non-Newtonian pseudoplastic crude oil and water flow inside horizontal pipes simulated by ANSYS. The study helps predict velocity and velocity profiles, as well as pressure drop during two-phase crude-oil−water flow, without complex calculations. Computational fluid dynamics (CFD) analysis will be very important in reducing the experimental cost and the effort of data acquisition. Three independent horizontal stainless steel pipes (SS-304) with inner diameters of 1 in., 1.5 in., and 2 in. were used to circulate crude oil with 5, 10, and 15% v/v water for simulation purposes. The entire length of the pipes, along with their surfaces, were insulated to reduce heat loss. A grid size of 221,365 was selected as the optimal grid. Two-phase flow phenomena, pressure drop calculations, shear stress on the walls, along with the rate of shear strain, and phase analysis were studied. Moreover, velocity changes from the wall to the center, causing a velocity gradient and shear strain rate, but at the center, no velocity variation (velocity gradient) was observed between the layers of the fluid. The precision of the simulation was investigated using three error parameters, such as mean square error, Nash-Sutcliffe efficiency, and RMSE-standard deviation of observation ratio. From the simulation, it was found that CFD analysis holds good agreement with experimental results. The uncertainty analysis demonstrated that our CFD model is helpful in predicting the rheological parameters very accurately. The study aids in identifying and predicting fluid flow phenomena inside horizontal straight pipes in a very effective way.

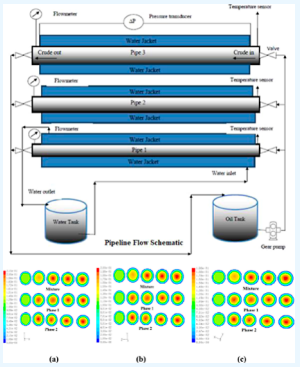

1. INTRODUCTION

Transporting crude oil from remote sources to refineries poses significant challenges, primarily when dealing with heavy crude oil. This transportation relies on pipelines with powerful pumps, but it encounters issues such as pressure loss and friction-induced deceleration or acceleration.[1] To mitigate these challenges, a common approach involves mixing the heavy crude oil with water, which reduces viscosity and aids in transportation. However, this introduces complexity through multiphase oil−water flow, where various parameters like the velocity of the mixture, transport pipe diameter, temperature, volume fraction, and pressure significantly impact the flow behavior. Furthermore, the substantial viscosity difference between crude oil and water complicates this process, necessitating careful engineering considerations for efficient and safe transportation of crude oil over long distances from its remote sources to processing facilities.[2]

Computational modeling and analysis of two-phase crude oil−water systems may enhance our present knowledge related to the transport mechanisms of oil−water mixtures in pipelines. The mainstream experimental and research work on two-phase oil−water flow focuses on flow pattern identifications such as intermittent, stratified, dispersed, core-annular, and the amalgamation of all the above.[3,4] However, computational modeling and analysis, like 3D computational fluid dynamics (CFD), have grown over the years as very important simulation tools due to their flexibility and cost-effectiveness for in-house studies.[5] The application of the CFD-based solver ANSYS for single and two-phase crude oil flow through pipes has been utilized by Kumar et al.,[6] Parvini et al.,[7] and Walvekar et al.[8] Pouraria et al.[9] applied CFD-based models for determining the flow patterns of oil−water. They utilize a general *k*-epsilon turbulence model in conjunction with the Eulerian−Eulerian method. The numerical results acquired were juxtaposed with experimental data found in the literature, focusing on either the in situ Sauter mean diameter or water volume fraction. The comparison between the

Received: July 21, 2023
Revised: January 23, 2024
Accepted: February 9, 2024
Published: March 1, 2024

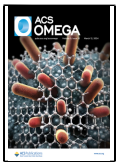

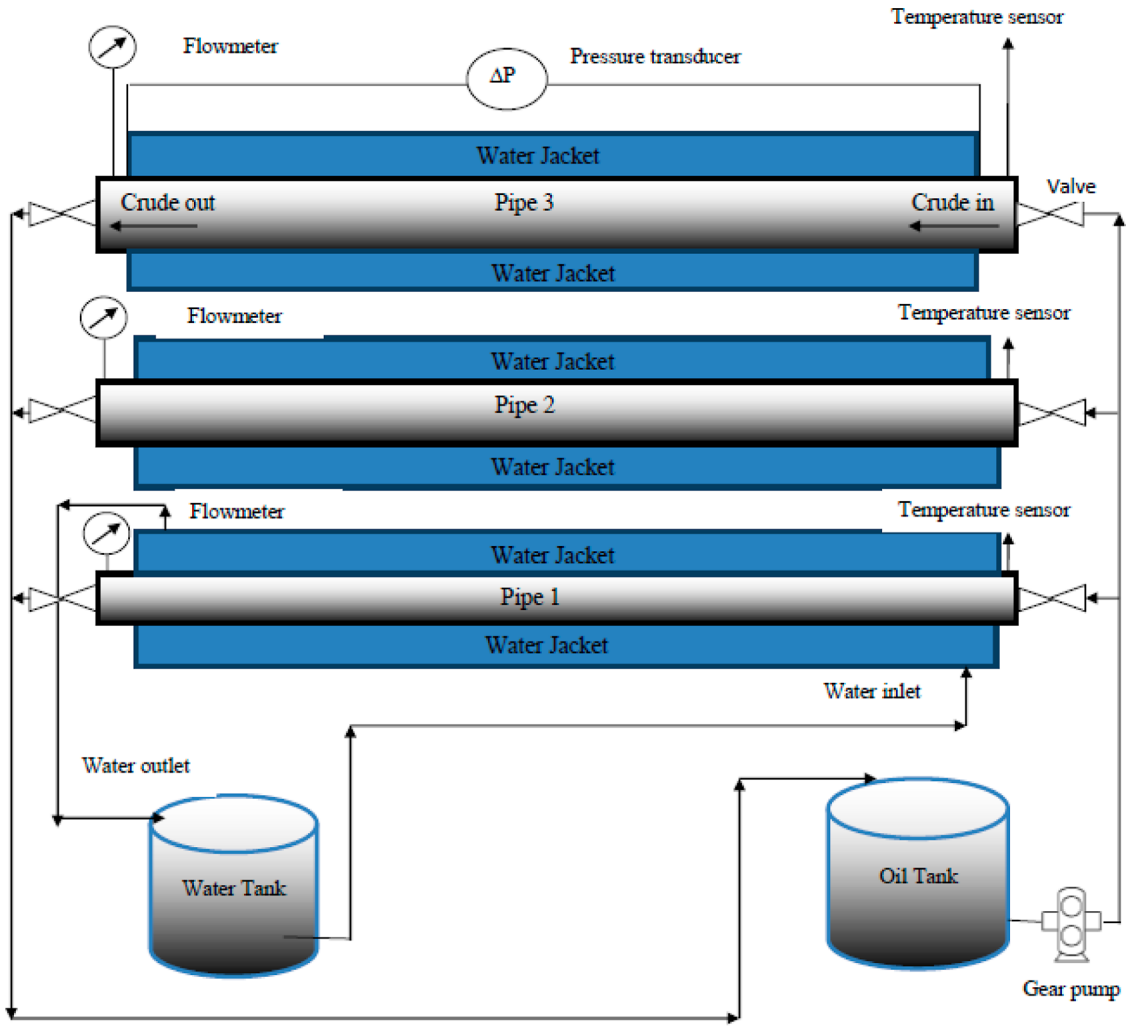

Pipe 1: length (test section) = 2.5 m
diameter = 0.0254 m
relative roughness = 0.00059

Pipe 2: length (test section) = 2.5 m
diameter = 0.0381 m
relative roughness = 0.000393

Pipe 3: length (test section) = 2.5 m
diameter = 0.0508 m
relative roughness = 0.000295

Figure 1. Schematic of the experimental setup for pipeline studies.

numerical findings and the previously published experimental data revealed a satisfactory level of agreement. Similarly, Bannwart[10] developed a suitable model for investigating aspects of oil−water core annular flow. In that study, mass and momentum-balanced phenomenological models were exploited to investigate volume fractions and changes in pressure. The predicted outcomes were weighted against vertical and horizontal oil−water core annular flows. The study demonstrated that predicted values followed the actual ones with high accuracy. Bandyopadhyay and Das[11] investigated non-Newtonian fluid flow and proposed empirical correlations for different piping components. They conducted experiments to estimate the frictional pressure drop across various piping components for non-Newtonian pseudoplastic flow under laminar conditions. They proposed an empirical correlation model for pronouncing frictional pressure drop in physical and dynamic variable forms. Castro-Gualdrón et al.[12] incorporated CFD techniques for simulating the homogenization of crude oil on a small scale. The effect of the mesh size and time step size was studied since, in this type of simulation, computational effort became a major parameter that had to be reduced to a minimum. Experimental data taken from two different points in the tank at regular time intervals was available to compare the results of the simulations, concluding in good agreement.

https://doi.org/10.1021/acsomega.3c05290
ACS Omega 2024, 9, 11181−11193

Desamala et al.[13] conducted a detailed CFD study of two-phase oil−water flow characteristics inside horizontal pipes. The simulation successfully predicted slug, stratified wavy, stratified mixed, and annular flow, with the exception of the dispersion of oil in water and the dispersion of water in oil. Simulation results were validated with horizontal literature data, and good conformity was observed. Abed and Auda[14] conducted an experimental and simulation study of oil−water flow inside the horizontal pipe to investigate heat transfer effects on the same. Yuan et al.[15] suggested a novel real-gas model for characterizing and predicting gas leakage in pipelines where gas is flowed at high pressures. They derived thermodynamic formulas based on the basic governing equations and concluded that the newly derived model worked better than the previous models in the same fields of study. Wang et al.[3] simulated flow behaviors of heavy oils in pipelines and predicted mesoscopic flow with the drag force model and KTGF models. From their experimental and modeling results, the filtered model was adopted for the flow as it provided better accuracy. Zhang et al. developed a VOF-DEM model for studying the particle dynamic behaviors in fractured-vuggy reservoirs. They predicted that the injection velocity, particle volume fraction, and diameter may alter the accumulation of particle plugging agents and affect channel flow control.[16] Saleh et al.[17] investigated the flow of heavy crude oil through pipelines using CFD. They used Ansys Fluent software for the study of the rheological flow behavior of Iraqi oil and found that the developed model was on par with the experimental results. Meriem-Benziane et al.[18] used CFD to study oil−water flow in a pipeline and their boundary layer separation investigation. Their analytical analysis was in good agreement with the numerical investigations. Songyi et al.[19] suggested a novel model for predicting the dependence of the shape of the interface between oil and water on their stratified flow. To solve the momentum equations, they used contact angle theory and the minimum energy method. Ballesteros et al.[20] used CFD to study the liquid holdup characteristics in a two-phase low liquid-loaded flow. Their investigation implied that smooth flow was possible using pipe inclination in the downward direction, while a lesser liquid holdup was seen for the same. Alade[21] introduced two new models, namely Cross-Logistic and Logistic, along with CFD, to study the complex flow behavior of crude oil and bitumen-solvent mixtures for using them to flow through porous media. Shadloo et al.[22] used an artificial neural network to estimate the pressure drop for the 2-phase flow of crude oil through long horizontal pipes using the experimental data for the same. Their findings suggested that their model predicted the pressure drop with much more accuracy than other empirical models employed for the same. Zheng et al.[23] used response surface methodology and sensitivity analysis to predict and optimize the viscosity of nano-oil containing ZnO2 nanoparticles.

The mentioned studies cover a broad spectrum of investigations on fluid flow and transport phenomena, offering valuable insights into various aspects of crude oil flow. Among them, the CFD model can offer detailed insights into crude oil behavior within pipelines, aiding researchers in understanding the impact of factors like viscosity, temperature, pressure, and flow rate on flow patterns, turbulence, and mixing. However, studies on the velocity profile, pressure drop, phase analysis, and flow pattern of crude oils through pipelines have not reached widespread research. In this regard, the current research investigates the phenomenon of non-Newtonian pseudoplastic crude oil−water mixture flow through horizontal pipes. The study includes the presence of water as a secondary phase in crude oil, which gives rise to complex phenomena like emulsion formation, which may affect the crude oil quality. The ANSYS Fluent CFD solver has been used to solve the flow structure, static pressure, pressure drop, friction factor, shear strain, and wall shear stress. These simulated results can be used for the optimum selection of design parameters for the horizontal pipelines used for transporting non-Newtonian crude oil−water flow. Information regarding the pumping cost of the crude oil−water flow through the pipeline can be gathered from the pressure drop analysis. The finding can contribute to the efficient identification and prediction of heavy crude flow phenomena within horizontal straight pipes.

2. EXPERIMENTAL DESCRIPTION

The experimental setup comprises an oil bath of 30 L volume containing a temperature regulator and mechanical impeller, a stainless steel double pipe heater, a gear pump (DFD), valves for the regulation of crude oil flow, and thermocouples for temperature reading. The test segment comprises three horizontal independent stainless steel pipes (SS-304) of 0.0508 m or 2 in. (relative roughness (ε/d) = 0.000295), 0.0381 m or 1.5 in. (relative roughness (ε/d) = 0.000393), 0.0254 m or 1 in. diameter (relative roughness (ε/d) = 0.00059), and 2.5 m length (Figure 1). The relative roughness was measured by dividing the roughness ε of the pipe by the diameter. The value of epsilon ε was provided by the manufacturer, while the internal diameter was calculated using calipers. The entire pipeline and exposed surfaces are totally insulated for minimizing the loss of heat. The crude oil as already mentioned, is collected from the western oilfield of India. Circulation of the crude oil through pipes has been done by a gear pump (Moyno_ 500 Pumps, 600 series). The flow rate of crude oil through different pipelines is measured by a digital flow meter (Everest EMAG series). Pressure drop was measured by a pressure transducer (manufactured by Rosemount Co. series 3051s) that measures the pressure loss linked to the inlet and outlet at a distance of 2.5 m. Fluid was kept in circulation mode in anticipation of the loop reaching its stabilized state for different flow rates and temperatures. Temperature was maintained by a shell and tube heat exchanger. A thermocouple (J-type, ThermoSensors) was placed in the middle of the flow line to measure temperature. All the experiments have been run at four different temperatures of 25−40 °C. The relay section comprised flow meters, pressure transducers, and temperature sensors, all relaying to a control panel through which the set values were adjusted. Water was added to the crude oil in the crude oil bath in different proportions and mixed thoroughly using a stirrer. A de-emulsifier was added to the mixture to prevent emulsion formation. The heated water from the water bath was circulated inside the jackets to make sure all the waxes or crude oils stuck in the inner walls of the pipelines were removed after the completion of each experiment.

33. COMPUTATIONAL FLUID DYNAMICS

CFD is an approach that uses algorithms to obtain extremely accurate outcomes by considering various phenomena, such as fluid dynamics and mass transfer.[24,25] In this study, a fully developed length is assumed for model development to reduce costs. Optimal computer memory has been utilized for grid

https://doi.org/10.1021/acsomega.3c05290
ACS Omega 2024, 9, 11181−11193

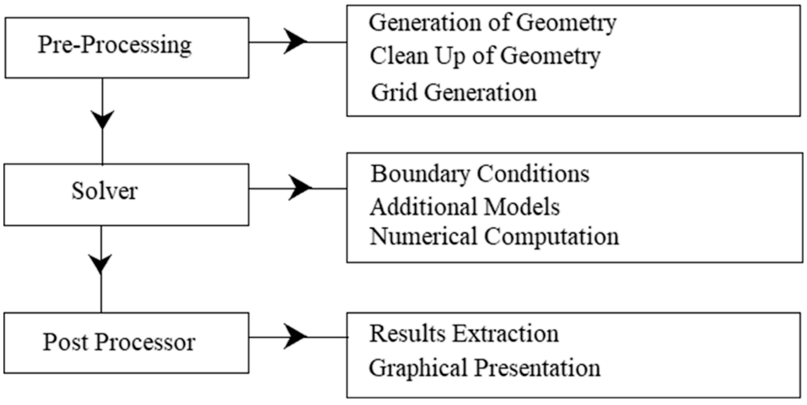

Figure 2. General steps involved in CFD analysis.

generation, which reduces convergence time during the simulation process. Initial investigations indicated laminar flow since the Reynolds number was found to be less than 2300. Non-Newtonian pseudoplastic crude oil−water flow through a horizontal pipe is a highly multifaceted study and is usually governed by the continuity and momentum equations in laminar flow. The continuity and momentum equations can be defined as eqs 1 and 2, respectively

$$\frac{\mathrm{d}}{\mathrm{d}t}(\alpha_i\rho_i) + \nabla\cdot(\alpha_i\rho_i u_i) = \sum_{j-1}^{N} m_{ij} \tag{1}$$

$$\frac{\mathrm{d}}{\mathrm{d}t}(\alpha_i\rho_i u_i) + \nabla\cdot(\alpha_i\rho_i u_i u_i) = -\alpha_i\nabla p + \alpha_i\rho_i g + \nabla\bar{\bar{\tau}}_i + \sum_{j=1}^{N}(R_{ij} + m_{ij}u_i) + \alpha_i\rho_i\cdot(F_i + F_{\mathrm{lift},i} + F_{\mathrm{vm},i}) \tag{2}$$

In eq 1, α_i = fraction for the ith phase; ρ_i = density of the ith phase; ∇ = nabla, defined as

$$\nabla = i\frac{\mathrm{d}}{\mathrm{d}x} + j\frac{\mathrm{d}}{\mathrm{d}y} + k\frac{\mathrm{d}}{\mathrm{d}z}$$

and u_i = velocity of the ith phase, ms^{-1}; m_{ij} = mass flow rate, kg s^{-1}.

In eq 2, g = acceleration due to gravity, ms^{-2}; $\bar{\bar{\tau}}_i$ = stress−strain tensor of the ith phase; R_{ij} = interaction force between the phases, N; F_i = external body force, N; F_{lift} = lift force, N; F_{vm} = virtual mass force, N. The interphase exchange force can be defined by eq 3

$$R_{ij} = K_{ij}\cdot(u_j - u_i) \tag{3}$$

where K_{ij} = fluid−fluid exchange coefficient. The flow being laminar, the power law model was selected as the viscous model, and the mixture model was selected for the multiphase model for CFD simulation.

The rheology of crude oil−water flow is found to be reliant on the apparent viscosity of the fluid flowing through the horizontal pipe. From the study, it has also been found that apparent viscosity depends on velocity and shear rate. The apparent viscosity of the crude oil−water mixture reduces with the increase in flow velocity and shear strain rate. The fluid inside the horizontal pipe follows the non-Newtonian pseudoplastic power law model. The apparent viscosity of a non-Newtonian fluid is given as eq 4

$$\mu_{\mathrm{app}} = K'\left(\frac{8u}{d}\right)^{n-1} \tag{4}$$

where μ_{app} is apparent viscosity, which is expressed in (Pa s). The boundary conditions were that the inlet and outlet of the pipes were considered to be velocity inlet and pressure outlet, respectively. Figure 2 shows the general steps involved in CFD simulation.

3.1. Assumption. To simulate the flow inside the pipe, the following assumptions and concepts were taken into consideration for the current study:

- The temperature of the crude oil−water mixture through the horizontal pipes was maintained at 25 to 40 °C.
- Crude oil−water is assumed to be incompressible and an isothermal non-Newtonian pseudoplastic fluid (The composition of crude oil makes it non-Newtonian as it includes suspended particles, saturates, aromatics, resins, asphaltenes, etc. Moreover, the shear stress-shear rate plot confirmed the crude oil as a pseudoplastic fluid).
- The model that has been developed is limited to a flow model (not a density model or a segregation model, etc.).
- The model is assumed to follow a two-phase laminar, non-Newtonian pseudoplastic power law model.

We assume no-slip conditions at the walls (to showcase the minimum velocity adjacent to the wall as a result of the high adhesive force between the pipeline wall and the fluid molecule as opposed to the center of the pipe).

3.2. Computational Approach, Convergence Criteria, and Grid Independency Test. Gambit 2.4.6 was utilized to generate a 3D tetrahedral grid geometry due to its excellent modeling flexibility and its ability to easily perform mesh skewness tests with minimal deviation. The boundary conditions and the continuum are specified within the geometry. The skewness of the tetrahedral grid was thoroughly examined, and it was found to be below 0.9. To get the simulated results, the geometries are exported to the CFD pressure-based solver (Fluent 6.3). To streamline the CFD procedures, a first-order upwind scheme is employed for the solution, and a simple pressure−velocity coupling is selected with relaxation.

Criteria of convergence were selected to be 10^{-5} for all the equations except the transport equation (whose convergence

https://doi.org/10.1021/acsomega.3c05290
ACS Omega 2024, 9, 11181−11193

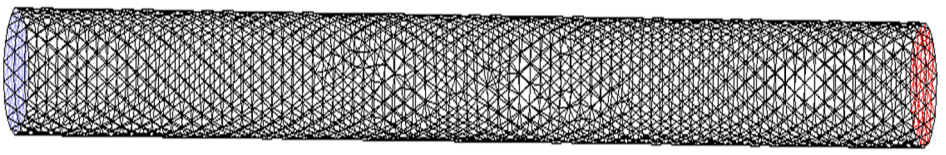

Figure 3. Tetrahedral mesh of the horizontal straight pipe.

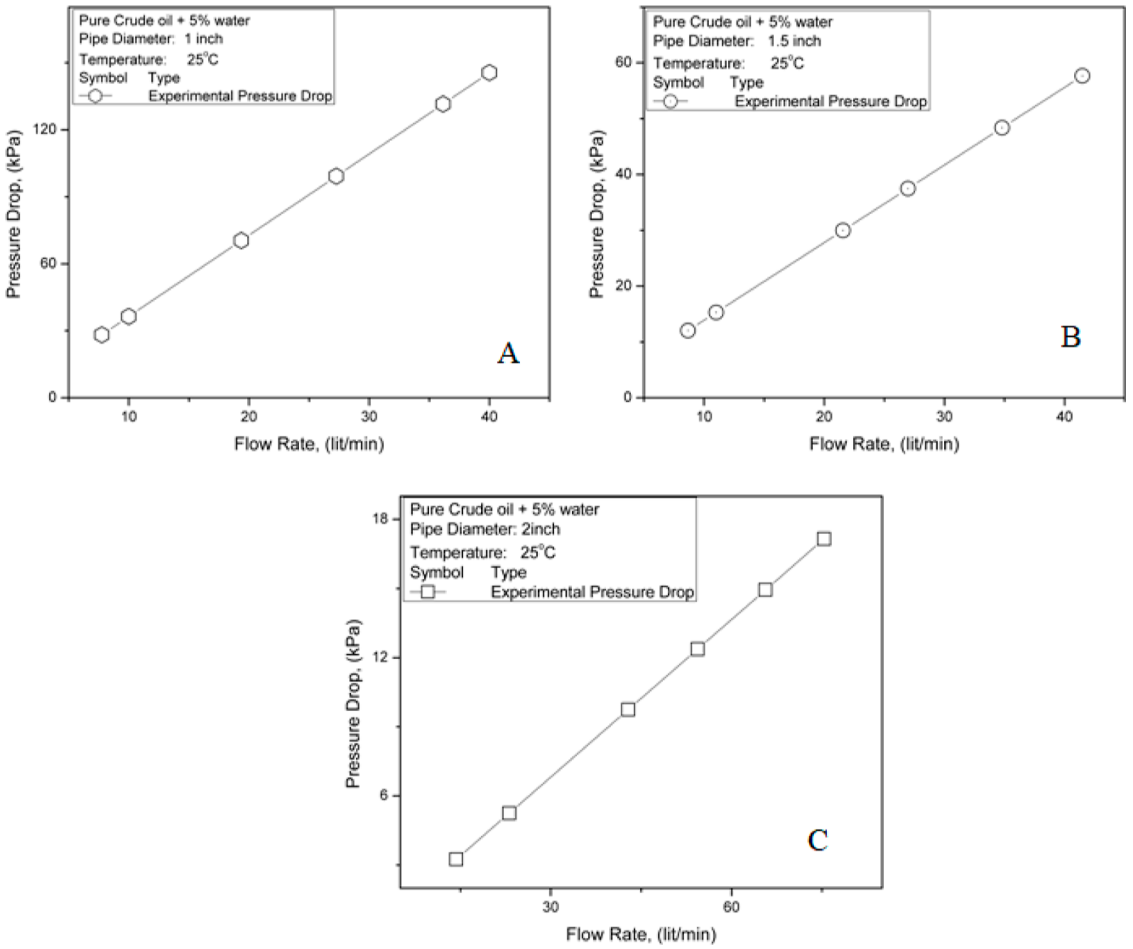

Figure 4. Comparative plot between pressure drop (kPa) and flow rate (L/min) for different pipe diameters (A) 1 in., (B) 1.5 in., and (C) 2 in.

criteria is 10^{-3}). The domain of computation (Lf = 0.05id) was selected for the laminar, fully developed flow through the various diameters of straight horizontal pipes. The test for grid independence is a function of the grid geometry of the pipelines. The concluding outcome of grid independence indicated 3−5% errors in pressure drop and velocity. A grid size of 221,365 was used for optimized grid results from the grid independence test (Figure 3). The results of CFD were on par with the data obtained from experiments.

3.3. Procedures for CFD. The general procedural steps to simulate the two-phase crude oil−water flow through different pipes are outlined below:

A Meshing of geometry using Gambit 6.3
- a Preparing a computational domain for the defined flow region.
- b Meshing of the geometry done by implementing boundary layer hexahedral and tetrahedral meshes.
- c Implementing a size function to allow smooth transitions in mesh size.
- d Defining boundaries and types of continuum.
- e Examined meshes to ensure that the skewness value is below 0.5 and 0.9 for hexahedral and tetrahedral meshes, respectively.

B Importing the mesh file to Fluent 6.3 and investigating the mesh

C Defining an unsteady, implicit, and pressure-based solver.

D Implementing a two-phase laminar non-Newtonian power law model.

E Activating the crude oil and water properties with laminar flow conditions.

F Enabling the operating conditions by activating gravity and defining the operating density.

G Methodology for solution control
- a Under relaxation factors of 0.5 and 0.3 for pressure and momentum, respectively, and default values were considered for other parameters.
- b Implementing a first-order upwind scheme for obtaining the solutions.
- c Activating simple pressure−velocity coupling.

https://doi.org/10.1021/acsomega.3c05290
ACS Omega 2024, 9, 11181−11193

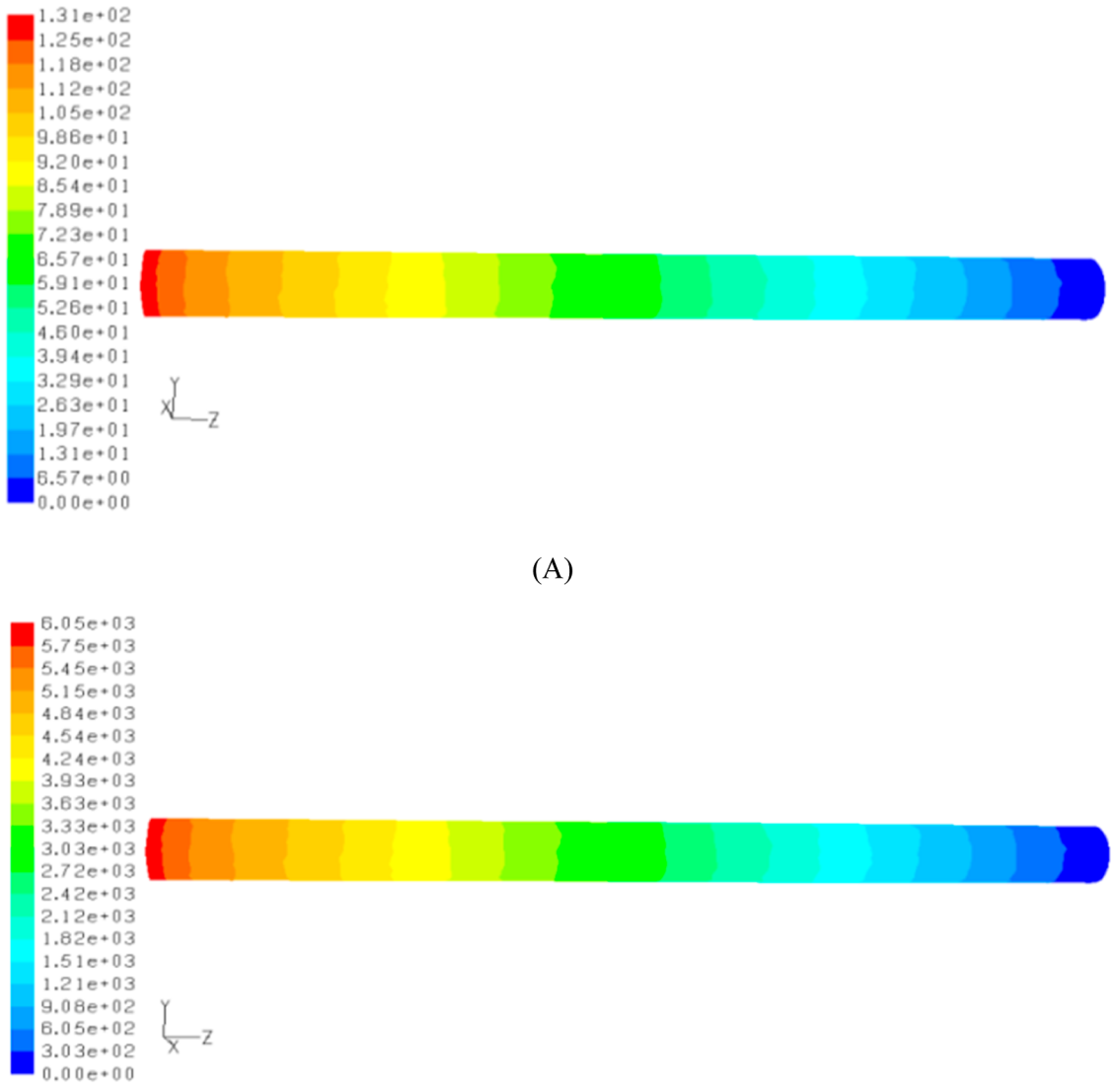

Figure 5. Contour of static pressure (Pa) for crude oil−water flow through a 2 in. horizontal pipe at 25 °C and velocity: (A) 0.11 m/s and (B) 0.62 m/s.

H Solution initialization: activating the residual plotting during the calculation, and enabling the default convergence criteria of 10^{-5} for all residuals except for the transport equation, which was selected to be 10^{-3}.

4. RESULTS AND DISCUSSIONS

4.1. Effect of Diameter on Pressure Drop. An important parameter that affects pressure drop is the pipe diameter and the relative roughness of the pipe (ε/d). Higher relative roughness leads to an increase in the skin friction factor. It is obvious that local turbulence near the surface of the pipeline changes with pipe relative roughness, and that would affect the thickness of the viscous sublayer. Therefore, when the thickness of the viscous sublayer becomes equal to or greater than the pipe roughness, the pipes are considered hydrodynamically smooth. The experimental results on the effect of pipe diameter on the drop in pressure for the flow of crude oil through different pipelines are shown in Figure 4A−C. The results indicate that pressure drop decreases with increasing pipe diameter when other parameters are fixed. The reduction in pressure drop was from about 125−42.5 kPa at a flow rate of 40 LPM under the same temperature conditions. This is attributed to the fact that huge eddy currents exist in the pipes with larger diameters, absorbing more energy from the main flow. In smaller pipelines, several small eddy currents are formed, whereas for larger-diameter pipes, the number of large eddies will be greater.

4.2. Effect of Velocity. The velocity profiles of crude oil flow through pipelines were calculated using the results obtained from pressure drop analysis during experimental investigations. Figure 5A,B illustrates the contour of static pressure (Pa), which increases with the increase in velocity of the crude oil−water through a horizontal pipe having a constant diameter (2 in.) operating at a constant temperature (25 °C). Pressure drop analysis showed that the change in pressure across the pipe increased with the inlet velocity of the fluid. The static pressure inside the pipe gradually decreases along the length of the pipe.

https://doi.org/10.1021/acsomega.3c05290
ACS Omega 2024, 9, 11181−11193

Figure 6A,B illustrates the velocity of the crude oil−water flow inside the horizontal straight pipe at 25 °C at every 0.5 m

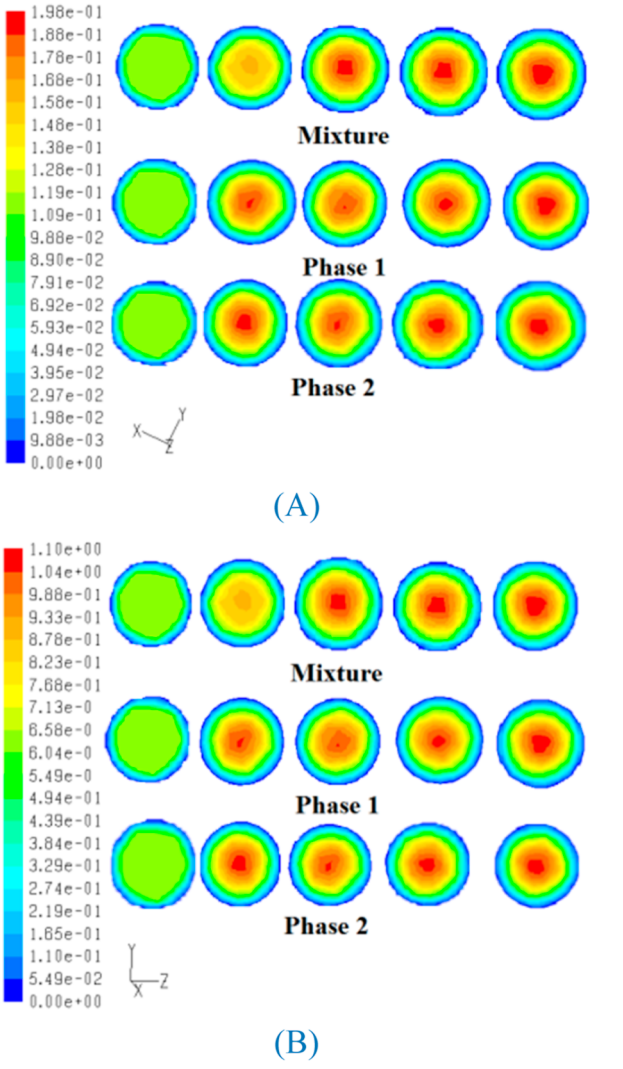

Figure 6. Contour of velocity (m/s) for crude oil−water flow at every interval of 0.5 m from the inlet through a 2 in. pipe at 25 °C and velocity: (A) 0.11 m/s (B) 0.62 m/s.

distance from the inlet. In the study, all the parameters like pipe diameter (2 in.), temperature, and concentration are kept constant, and the only parameter that has been varied is velocity. The study has been conducted for 2 dissimilar velocities (low = 0.11 m/s and high = 0.62 m/s). The study shows that the velocity of the fluid flow is at its maximum at the center and gradually decreases toward the wall. Adhesive force near the wall is maximum as compared to cohesive force.[26] This makes the velocity near the wall's minimum.

Figures 7 and 8 illustrate the contour of the wall shear stress and rate of shear strain for the crude oil−water mixture through the horizontal pipe at 25 °C at every 0.42 m interval from the inlet. It indicates that shear stress and strain rate are maximum near the wall and gradually decrease toward the center of the pipe. The velocity of the fluid at the wall is less because of friction between the pipe wall and the fluid, and hence drag is generated near the wall. The velocity of the adjacent layer fluid is changed up to the center from the wall, causing velocity distribution (shear strain = velocity gradient = $\frac{du}{dy}$). Therefore, velocity changes from the wall to the center, causing velocity gradient/shear strain rate. However, at the center, no velocity variation (velocity gradient) between the layers of the fluid is seen. This means velocity at the center is the maximum and unique. According to the Newtons law of viscosity, wall shear stress $(\tau) = \mu_{app} \times \left(\frac{du}{dy}\right)^n$, where n = flow behavior index, and μ_{app} is apparent viscosity. Hence, the shear stress of the fluid layer near the wall will be high and less at the center.

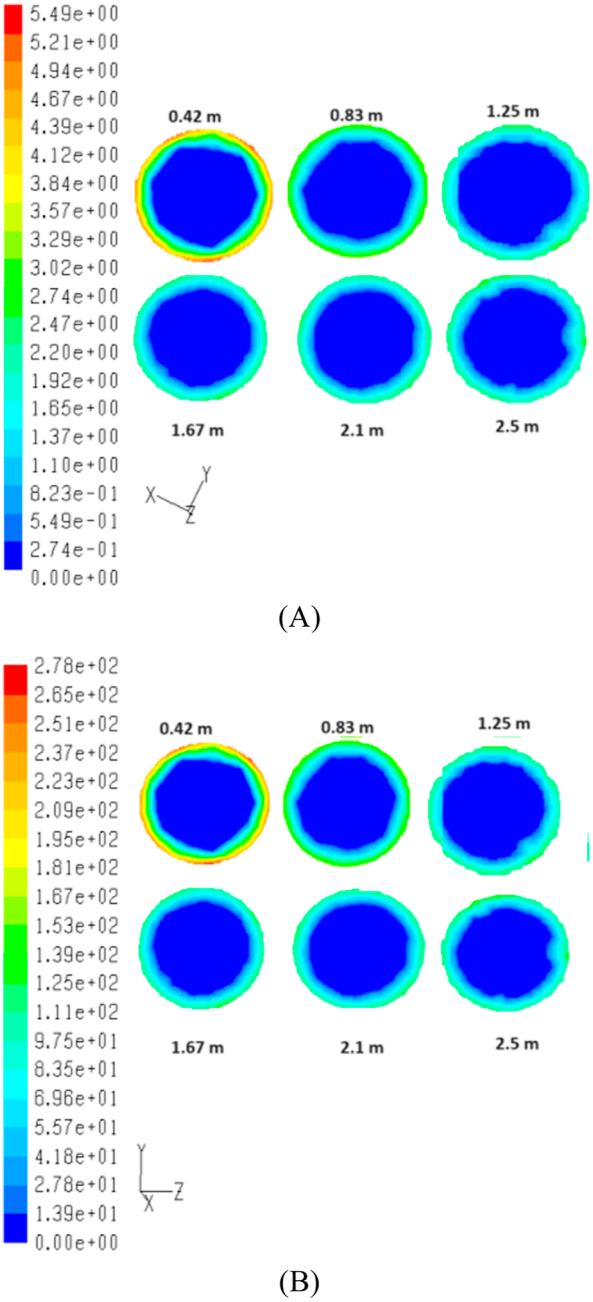

Figure 7. Contour of wall shear stress (Pa) for crude oil−water flow through a 2 in. horizontal pipe at every 0.42 m interval from the inlet at 25 °C and velocity: (A) 0.11 m/s and (B) 0.62 m/s.

4.3. Effect of Temperature. The effect of temperature on the non-Newtonian pseudoplastic crude oil−water fluid flow inside the 2 in. horizontal straight pipe was investigated. Figure

https://doi.org/10.1021/acsomega.3c05290
ACS Omega 2024, 9, 11181−11193

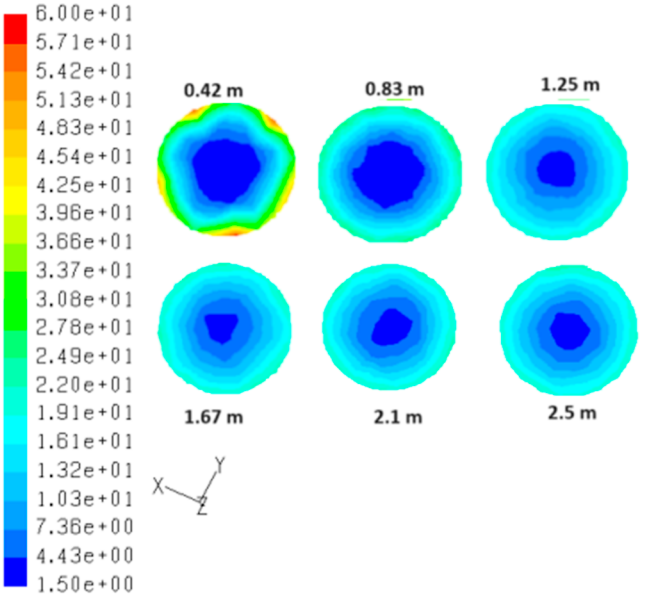

(A)

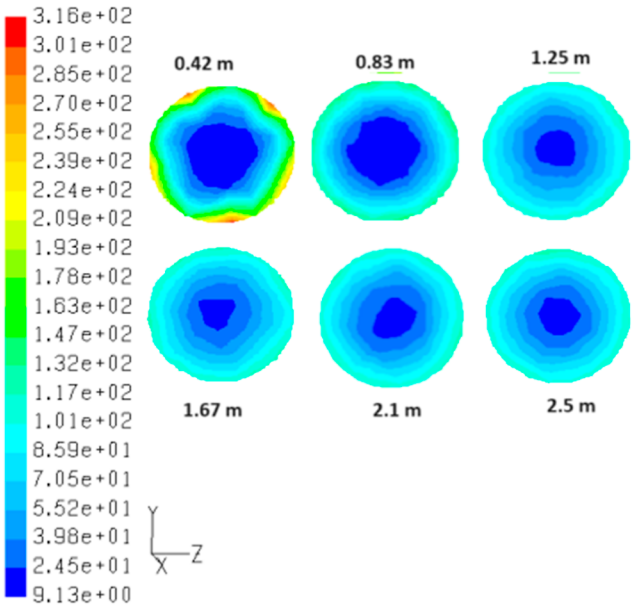

(B)

Figure 8. Contour of shear strain rate (s^{-1}) for crude oil−water flow inside the 2 in. horizontal straight pipe at every 0.42 m interval from the inlet at 25 °C and velocity (A) 0.11 m/s and (B) 0.62 m/s.

9 illustrates the contour plot of the static pressure of the crude oil−water flow inside the pipe. From the analysis, it is clear that the static pressure inside the horizontal straight pipe decreases with an increase in temperature. It was also observed that the static pressure reaches its maximum at 25 °C (0.1 kPa) and its minimum at 40 °C (0.06 kPa).

4.4. Effect of Pipe Diameter. Figure 10A−C depicts the contours of static pressure (Pa) for crude oil−water pseudoplastic non-Newtonian fluid flow inside various pipe diameters (1 in., 1.5 in., and 2 in.) operating at 25 °C, along with a constant velocity of 0.11 cm/s. The static pressure inside the pipe gradually decreases along the length of the pipe. The study also revealed that static pressure and pressure drop inside the horizontal straight pipe decrease with an increase in pipe diameter. The static pressure in the 1 in. horizontal straight pipe is found to be the maximum, and in the 2 in. horizontal straight pipe, it is the minimum.

Figure 11A−C indicates the contour of the velocity (m/s) inside the horizontal straight pipes of various diameters. From the contour, it has been found that pipe size affects the flow pattern inside the pipe. The velocity of the crude oil−water fluid flow decreases with an increase in pipe diameter, because at unvarying flow rates, velocity becomes inversely related to the cross-sectional area.

4.5. Phase Analysis. Figure 12 shows the phase analysis of crude oil−water flow through a 2 in. horizontal straight pipe at 25 °C at four equal intervals from the inlet. In this study, velocity, diameter, and temperature are kept constant, while the concentration of water is varied. The crude oil mostly accumulates in the midsection of the pipe due to the density difference, as seen in the figure. Since the density of the crude oil is lighter than that of the water, the crude oil remains in the midsection of the horizontal straight pipe. The bulk velocity of the fluid mixture strips the denser component (water) compared to the lighter component (crude oil) from the mixture toward the wall side as an exchange of momentum transfer. This results in the water being more concentrated toward the wall side and the crude oil at the center.

4.6. Comparison of Experimental and CFD Results. The results obtained from CFD were compared with experimental results in each pipeline and depicted in Table 1 and Figure 13A−C.

As seen in the figures, pressure drop increased with velocity in both the experimental and CFD work in each pipeline. Similarly, if we look at Table 1, there is a small difference between the experimental and simulated results (Figure 14). Maximum deviations were observed in the 2 in. diameter pipeline, while minimum deviations were observed in the 1 in. diameter pipeline. The deviation between experimental and simulated data is very small (i.e., <5%), which means that the simulated results and the flow equations used for simulation studies can properly predict the flow behavior of crude oil with minimal error. The results of velocity profile and flow patterns were also compared with various data reported in literature, as shown in Table 2. It is noteworthy that our CFD predictions exhibit a close match with the trends reported in the literature, affirming the predictive capability of our simulation methodology. This consistency lends credibility to our numerical approach and supports the validity of our findings.

4.7. Uncertainty Analysis. The precision of the developed CFD model was evaluated by implementing four error parameters, such as Nash-Sutcliffe efficiency (NSE), the RMSE-standard deviation ratio of observation (RMSE-standard deviation of the observation ratio (RSR)), and mean square error (MSE). The following error parameters can be estimated using eqs 5−7.[33,34]

$$\mathrm{NSE} = 1 - \frac{\sum_{i=1}^{n} (y_{i,\mathrm{act}} - y_{i,\mathrm{prd}})^2}{\sum_{i=1}^{n} (y_{i,\mathrm{act}} - y_{i,\mathrm{mean}})^2} \quad (5)$$

$$\mathrm{RSR} = \sqrt{\frac{\sum_{i=1}^{n} (y_{i,\mathrm{act}} - y_{i,\mathrm{prd}})^2}{\sum_{i=1}^{n} (y_{i,\mathrm{act}} - y_{i,\mathrm{mean}})^2}} \quad (6)$$

https://doi.org/10.1021/acsomega.3c05290
ACS Omega 2024, 9, 11181−11193

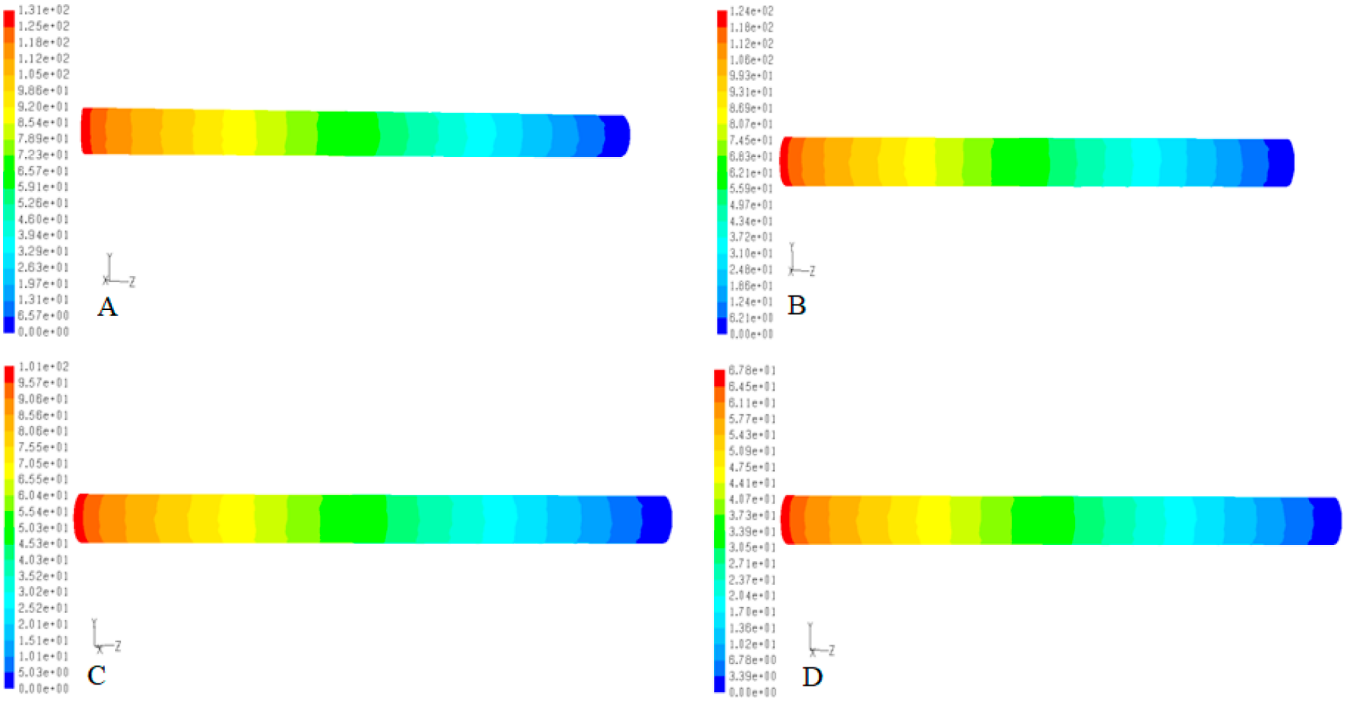

Figure 9. Contour of static pressure (Pa) of non-Newtonian pseudoplastic crude oil−water flow inside the horizontal straight pipe of diameter 2 in., velocity of 0.11 m/s, and temperatures (A) 25, (B) 30, (C) 35, and (D) 40 °C.

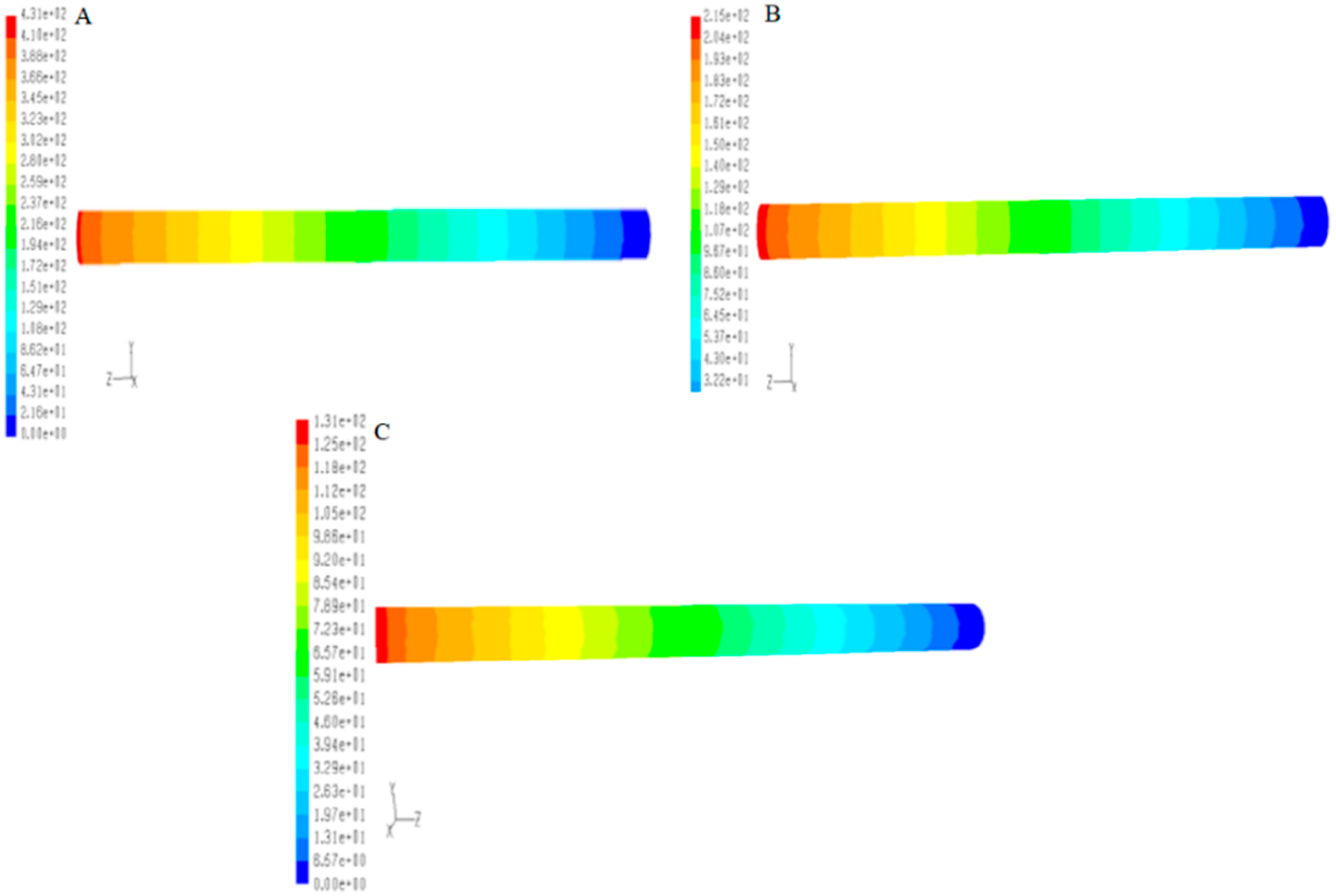

Figure 10. Contour of static pressure (Pa) of non-Newtonian pseudoplastic crude oil−water flow at 25 °C and velocity of 0.11 m/s and the diameter of the horizontal straight pipe (A) 1 in., (B) 1.5 in., and (C) 2 in.

https://doi.org/10.1021/acsomega.3c05290
ACS Omega 2024, 9, 11181−11193

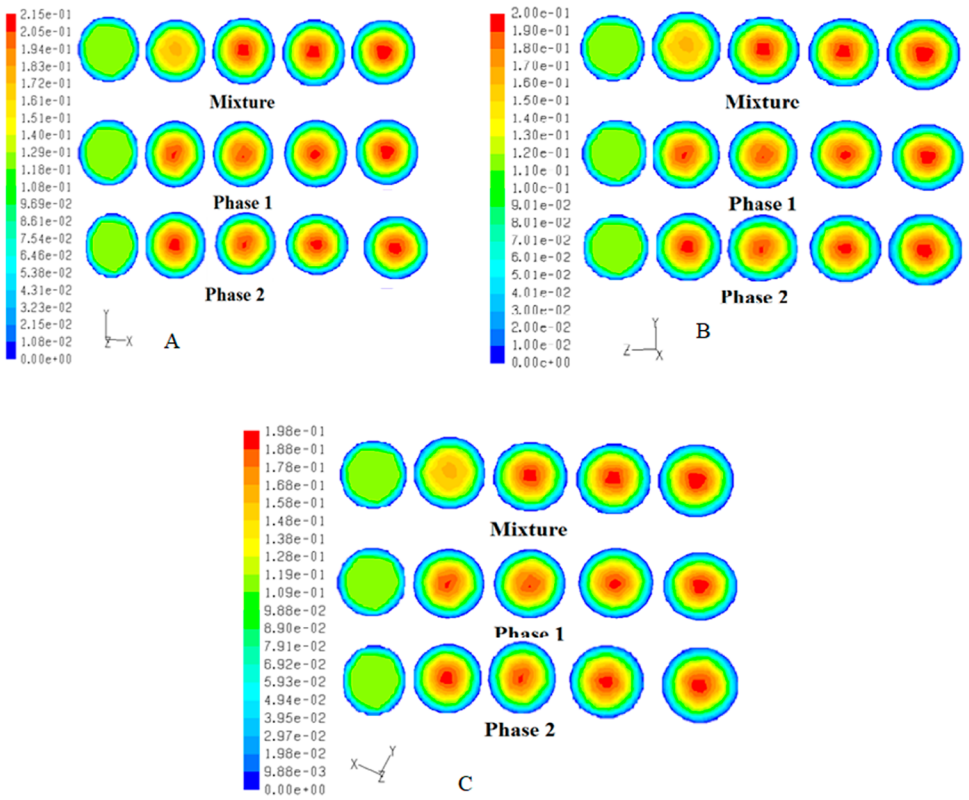

Figure 11. Contour of velocity (m/s) of non-Newtonian pseudoplastic crude oil−water flow at every 0.5 m intervals from the inlet at 25 °C and velocity of 0.11 m/s and diameter of the horizontal straight pipe (A) 1 in. (B) 1.5 in. (C) 2 in.

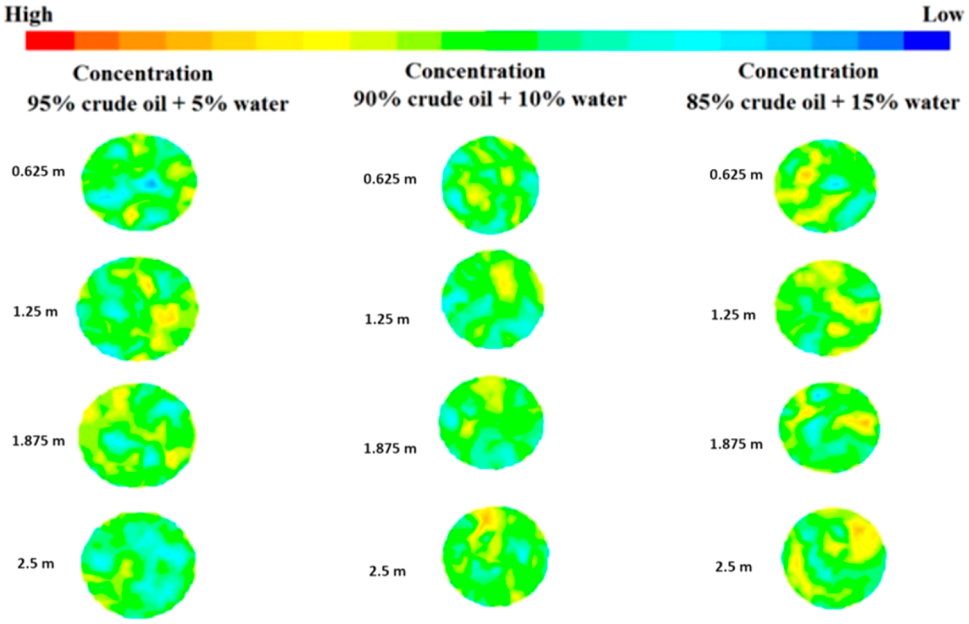

Figure 12. Contour of the crude oil−water fluid flow through a 2 in. straight horizontal pipe at every 0.625 m interval from the inlet at 25 °C and a velocity of 0.11 m/s.

$$\mathrm{MSE} = \frac{\sum_{i=1}^{n} (y_{i,\mathrm{act}} - y_{i,\mathrm{prd}})^2}{n} \quad (7)$$

In eqs 5−7, the experimental values and CFD predicted values are denoted by $y_{i,\mathrm{act}}$, and $y_{i,\mathrm{prd}}$, respectively. The mean of the experimental values is represented by $y_{i,\mathrm{mean}}$. The recommended best values of NSE, RSR, and MSE are 1, 0, and 0, respectively.[35] The calculated values are considered acceptable if they are found close to the best values. Table 3 shows the uncertainty analysis. The estimated values of all three error parameters are close to the best, demonstrating the model's acceptability and accuracy. Moreover, the total error values for three pipe diameters (1 in., 1.5 in., and 2 in.) models show a similar trend, and the values demonstrate very less

https://doi.org/10.1021/acsomega.3c05290
ACS Omega 2024, 9, 11181−11193

Table 1. Comparison between Experimental and Simulated Data

condition	velocity (cm/s)	pressure drop (kPa)		deviation (%)
		experimental	CFD	
pure crude +5% water, pipe dia: 2″, temp: 25 °C	11.75	3.25	3.37	3.56
	18.98	5.251	5.5	4.54
	35.26	9.751	9.93	1.81
	44.72	12.37	12.7	2.37
	54.01	14.94	15.1	1.13
	62.02	17.15	17.4	1.21
pure crude +5% water, pipe dia: 1″, temp: 25 °C	25.52	28.22	28.3	0.42
	32.92	36.4	36.6	0.44
	63.71	70.46	70.7	0.37
	89.77	99.29	99.4	0.15
	119	131.6	132	0.11
	131.7	145.6	146	0.13
pure crude +5% water, pipe dia: 0.5″, temp: 25 °C	17.63	8.664	8.77	1.25
	22.39	11.01	11.2	1.61
	43.89	21.57	21.7	0.69
	54.86	26.97	27.1	0.52
	70.79	34.8	35	0.49
	84.4	41.49	41.7	0.43

deviation from each other. Thus demonstrating the stability and accuracy of the developed CFD model.

5. CONCLUSIONS

This extensive investigation delved into the complex dynamics of non-Newtonian pseudoplastic mixtures of crude oil and water as they traverse horizontal pipes. The study provided valuable insights into critical factors such as pipe diameter, velocity, and temperature, elucidating their profound impact on flow patterns and pressure drop. Utilizing CFD, specifically the ANSYS Fluent solver, proved essential for simulating and analyzing these intricate fluid behaviors. The research revealed key findings: larger pipes exhibited reduced pressure drop due to the formation of more substantial eddies, velocity profiles displayed a peak at the pipe center diminishing toward the wall, influenced by adhesive forces, and temperature fluctuations affected static pressure, with higher temperatures resulting in lower static pressure. Phase analysis uncovered water's affinity for the wall and crude oil's concentration in the center. Comparison with experimental data confirmed the CFD model's accuracy, with deviations below 5%, and uncertainty analysis affirmed the model's reliability. Additionally, the predicted flow pattern from CFD aligned well with the existing literature.

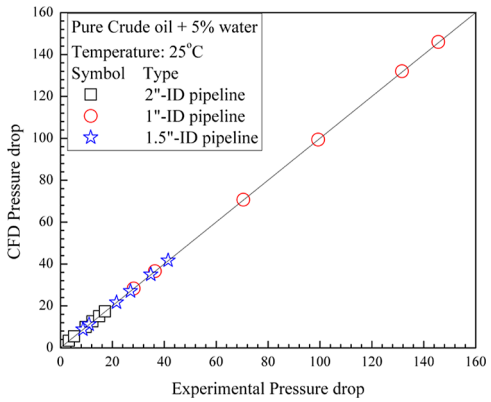

Figure 14. Comparison of experimental and CFD pressure drop.

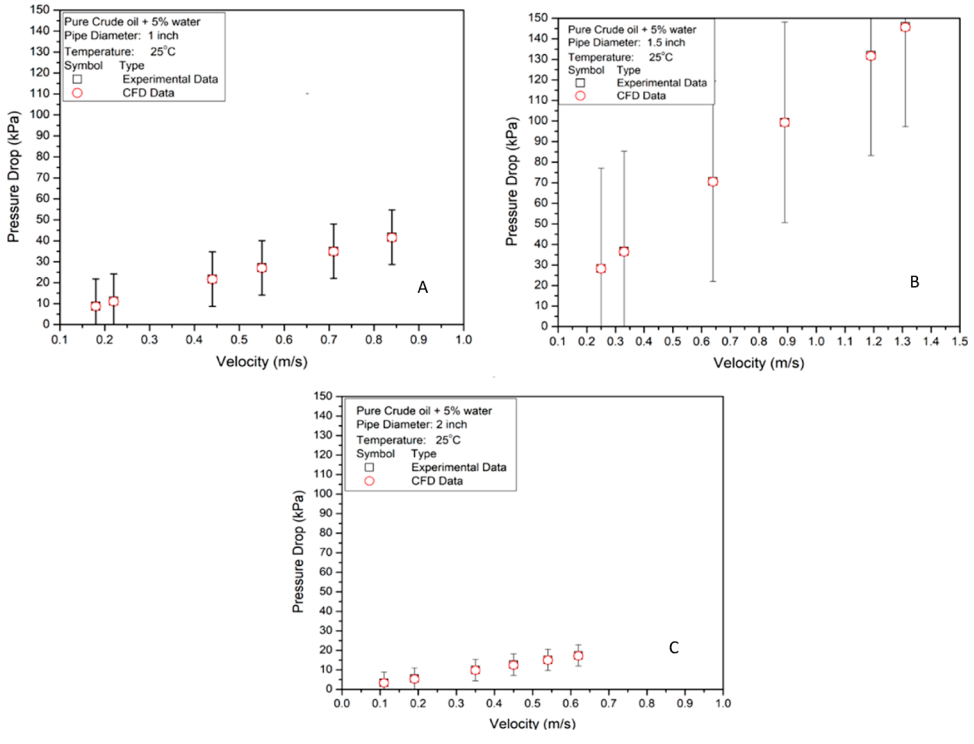

Figure 13. Comparison of pressure drop and velocity between experimental and CFD data: (A) 1 in., (B) 1.5 in., and (C) 2 in.

https://doi.org/10.1021/acsomega.3c05290
ACS Omega 2024, 9, 11181−11193

Table 2. Prior Experimental Investigations Concerning the Flow of Oils in Horizontal Pipes with Oil−Water Mixtures

author	pipe material	flow orientation	density (kg/m^3)	viscosity (mPa s)	ID (m)	measured parameters	reference
Mukherjee et al.	metal	vertical and horizontal	850	3.5	0.0381	pressure gradient and holdup	27
Abduvayt et al.	St-steel	vertical and horizontal	800	1.88 ± 0.19	0.1064	flow pattern, holdup, and pressure drop	28
Soleimani	St-steel		801	1.6	0.0243	flow pattern, and pressure drop	29
Kumara et al.	steel	−5° ∼ + 5°	790	1.64	0.056	flow pattern, local water fraction, and pressure drop	30
Alkaya et al.	acrylic		849	12.9	0.0501	flow pattern, holdup, and pressure drop	31
Rodriguez and Oliemans	steel	horizontal	830	7.5	0.0828	flow pattern, holdup, and pressure drop	32

Table 3. Uncertainty Analysis

models	NSE	RSR	MSE	total error value
1 in. diameter pipe	0.99	0.014	0.028	1.03
1.5 in. diameter pipe	0.99	0.0061	0.073	1.07
2 in. diameter pipe	0.99	0.045	0.051	1.08

Future studies in this domain could focus on exploring the impact of varying parameters such as pipe roughness, fluid rheology, and composition on the observed phenomena. Investigating the behavior of multiphase flow under different operational conditions, such as varying pressures and temperatures, could provide a more comprehensive understanding. Furthermore, studies assessing the scalability of the findings to real-world pipeline systems and the development of improved modeling approaches for even more accurate predictions would contribute to the continued advancement of knowledge in crude oil−water transport dynamics.

■ ASSOCIATED CONTENT

Supporting Information

The Supporting Information is available free of charge at https://pubs.acs.org/doi/10.1021/acsomega.3c05290.

Pressure drop, flow rate, and viscosity values of crude oil flow through different pipes (XLSX)

■ AUTHOR INFORMATION

Corresponding Authors

Shirsendu Banerjee − *School of Chemical Technology, Kalinga Institute of Industrial Technology, Bhubaneswar 751024, India;* orcid.org/0000-0001-9559-3192; Email: shirsendu.banerjee@kiitbiotech.ac.in

Byong-Hun Jeon − *Department of Earth Resources & Environmental, Engineering, Hanyang University, Seoul 04763, Republic of Korea;* orcid.org/0000-0002-5478-765X; Email: bhjeon@hanyang.ac.kr

Suraj K. Tripathy − *School of Chemical Technology, Kalinga Institute of Industrial Technology, Bhubaneswar 751024, India;* Email: suraj.tripathy@kiitbiotech.ac.in

Authors

Anirban Banik − *Department of Civil Engineering, NIT Sikkim, Ravangla, Sikkim 737139, India*

Vinay Kumar Rajak − *Department of Petroleum Engineering, Indian Institute of Technology (Indian School of Mines) Dhanbad, Dhanbad, Jharkhand 826004, India*

Tarun Kanti Bandyopadhyay − *Department of Chemical Engineering, NIT, Agartala, Tripura 799046, India*

Jayato Nayak − *Centre for Life Sciences, Mahindra University, Hyderabad, Telengana 500043, India*

Michał Jasinski − *Department of Electrical Engineering Fundamentals, Wroclaw University of Science and Technology, Wrocław 50-370, Poland*

Ramesh Kumar − *Department of Earth Resources & Environmental, Engineering, Hanyang University, Seoul 04763, Republic of Korea*

Masoom Raza Siddiqui − *Chemistry Department, College of Science, King Saud University, Riyadh 11451, Saudi Arabia*

Moonis Ali Khan − *Chemistry Department, College of Science, King Saud University, Riyadh 11451, Saudi Arabia*

Sankha Chakrabortty − *School of Chemical Technology, Kalinga Institute of Industrial Technology, Bhubaneswar 751024, India;* orcid.org/0000-0001-7719-8586

Complete contact information is available at: https://pubs.acs.org/10.1021/acsomega.3c05290

Notes

The authors declare no competing financial interest.

■ ACKNOWLEDGMENTS

The authors express their gratitude to the School of Biotechnology and Chemical Technology, KIITUniversity, and the Chancellor, Vice-Chancellor, and Management of Mahindra University, Hyderabad, India, for the required infrastructure and visionary leadership. This work was supported by the National Research Foundation of Korea (NRF) grant funded by the Korea government (MSIT) (no. RS-2023-00219983). Moonis Ali Khan acknowledges the financial support through Researchers Supporting Project number: RSP2024R345, King Saud University, Riyadh. Saudi Arabia. One of the authors (R. Kumar) acknowledges the financial support through the National Research Foundation (NRF) of the Republic of Korea under the Creative and Challenging Research Program (2021R1I1A1A01060846).

■ NOMENCLATURE

α_i, fraction for the ith phase; ρ_i, density of the ith phase; ∇, $\nabla = i\frac{d}{dx} + j\frac{d}{dy} + k\frac{d}{dz}$; u_i, velocity of the ith phase, ms^{-1}; m_{ij}, mass flow rate, kg s^{-1}; g, Acceleration due to gravity, ms^{-2}; $\bar{\bar{\tau}}_i$, stress−strain tensor of the ith phase; R_{ij}, interaction force between the phases, N; F_i, external body force, N; F_{lift}, lift force, N; F_{vm}, virtual mass force, N; K_{ij}, fluid−fluid exchange coefficient; μ_{appp}, apparent viscosity, Pa s; $\frac{du}{dy}$, shear strain OR velocity gradient; n, flow behavior Index; $y_{i,\text{act}}$, experimental values; $y_{i,\text{prd}}$, CFD predicted values

https://doi.org/10.1021/acsomega.3c05290
ACS Omega 2024, 9, 11181−11193

GLOSSARY

CFD	computational fluid dynamics
RMSE	root mean square error
RSR	RMSE-observations standard deviation ratio
VOCs	volatile organic compounds
KTGF	kinetic theory of granular flow
VOF-DEM	volume of fluid-discrete element method
NSE	Nash-Sutcliffe efficiency

REFERENCES

(1) Niazi, S. CFD Simulation of a Crude Oil Transport Pipeline: Effect of Water. *Pet. Petrochem. Eng. J.* **2018**, *2* (3), 4−8.

(2) Burlutskii, E. CFD Study of Oil-in-Water Two-Phase Flow in Horizontal and Vertical Pipes,. *J. Pet. Sci. Eng.* **2018**, *162* (August 2017), 524−531.

(3) Wang, W.; Gong, J.; Angeli, P. Investigation on heavy crude-water two phase flow and related flow characteristics. *Int. J. Multiphase Flow* **2011**, *37*, 1156−1164.

(4) Xu, X. X. Study on Oil-Water Two-Phase Flow in Horizontal Pipelines,. *J. Pet. Sci. Eng.* **2007**, *59* (1−2), 43−58.

(5) Kaushik, V. V. R.; Ghosh, S.; Das, G.; Das, P. K. CFD Simulation of Core Annular Flow through Sudden Contraction and Expansion,. *J. Pet. Sci. Eng.* **2012**, *86*−*87*, 153−164.

(6) Kumar, R.; Banerjee, S.; Banik, A.; Bandyopadhyay, T. K.; Naiya, T. K. Simulation of Single Phase Non-Newtonian Flow Characteristics of Heavy Crude Oil through Horizontal Pipelines,. *Pet. Sci. Technol.* **2017**, *35* (6), 615−624.

(7) Parvini, M.; Dabir, B.; Mohtashami, S. A. Numerical Simulation of Oil Dispersions in Vertical Pipe Flow,. *J. Jpn. Pet. Inst.* **2010**, *53* (1), 42−54.

(8) Walvekar, R. G.; Choong, T. S. Y.; Hussain, S. A.; Khalid, M.; Chuah, T. G. Numerical Study of Dispersed Oil-Water Turbulent Flow in Horizontal Tube,. *J. Pet. Sci. Eng.* **2009**, *65* (3−4), 123−128.

(9) Pouraria, H.; Seo, J. K.; Paik, J. K. Numerical Modelling of Two-Phase Oil-Water Flow Patterns in a Subsea Pipeline,. *Ocean Eng.* **2016**, *115*, 135−148.

(10) Bannwart, A. C. Modeling aspects of oil-water core-annular flows. *J. Pet. Sci. Eng.* **2001**, *32*, 127−143.

(11) Bandyopadhyay, T. K.; Das, S. K. Non-Newtonian pseudo-plastic liquid flow through small diameter piping components. *J. Pet. Sci. Eng.* **2007**, *55*, 156−166.

(12) Castro-Gualdrón, J. A.; Abreu-Mora, L. A.; Díaz Mateus, F. A. CFD simulation of crude oil homogenization in pilot plant scale. *CT&F, Cienc., Tecnol. Futuro* **2013**, *5*, 19−30.

(13) Desamala, A. B.; Dasamahapatra, A. K.; Mandal, T. K. Oil-Water Two-Phase Flow Characteristics in Horizontal Pipeline - A Comprehensive CFD Study. In *International Journal of Chemical, Molecular, Nuclear, Materials and Metallurgical Engineering*; World Academy of Science, 2014; Vol. *8*, pp 336−340.

(14) Abed, E. M.; Auda, Z. A. Simulation and Experimental of Oil-Water Flow with Effect of Heat Transfer in Horizontal Pipe. *Int. J. Mech. Eng. Appl.* **2014**, *2*, 117−127.

(15) Yuan, F.; Zeng, Y.; Khoo, B. C. A New Real-Gas Model to Characterize and Predict Gas Leakage for High-Pressure Gas Pipeline,. *J. Loss Prev. Process. Ind.* **2022**, *74*, 104650.

(16) Zhang, T.; Zeng, X.; Guo, J.; Zeng, F.; Li, M. Numerical Simulation on Oil-Water-Particle Flows in Complex Fractures of Fractured-Vuggy Carbonate Reservoirs,. *J. Pet. Sci. Eng.* **2022**, *208*, 109413.

(17) Saleh, S. N.; Mohammed, T. J.; Hassan, H. K.; Barghi, S. CFD Investigation on Characteristics of Heavy Crude Oil Flow through a Horizontal Pipe,. *Egypt. J. Pet.* **2021**, *30* (3), 13−19.

(18) Meriem-Benziane, M.; Bou-Saïd, B.; Abdelkader, B. A CFD Modeling of Oil-Water Flow in Pipeline: Interaction Analysis and Identification of Boundary Separation. *Pet. Res.* **2021**, *6* (2), 172−177.

(19) Songyi, G.; Zhiming, W.; Quanshu, Z. A Novel Model for Oil-Water Stratified Flow in Horizontal Wells With a Curved Interface Based on Dynamic Contact Angle. *J. Energy Resour. Technol.* **2022**, *144* (2), 023003.

(20) Ballesteros, M.; Ratkovich, N.; Pereyra, E. ″Analysis and Modeling of Liquid Holdup in Low Liquid Loading Two-Phase Flow Using Computational Fluid Dynamics and Experimental Data.″. *J. Energy Resour. Technol.* **2021**, *143* (1), 012105.

(21) Alade, O. S. ″Rheological Modeling of Complex Flow Behavior of Bitumen-Solvent Mixtures and Implication for Flow in a Porous Medium.″. *J. Energy Resour. Technol.* **2022**, *144* (7), 073004.

(22) Shadloo, M. S.; Rahmat, A.; Karimipour, A.; Wongwises, S. ″Estimation of Pressure Drop of Two-Phase Flow in Horizontal Long Pipes Using Artificial Neural Networks.″. *J. Energy Resour. Technol.* **2020**, *142* (11), 112110.

(23) Zheng, Y.; Wang, S.; D'Orazio, A.; Karimipour, A.; Afrand, M. ″Forecasting and Optimization of the Viscosity of Nano-oil Containing Zinc Oxide Nanoparticles Using the Response Surface Method and Sensitivity Analysis.″. *J. Energy Resour. Technol.* **2020**, *142* (11), 113004.

(24) Pak, A.; Mohammadi, T.; Hosseinalipour, S. M.; Allahdini, V. CFD Modeling of Porous Membranes,. *Desalination* **2008**, *222* (1−3), 482−488.

(25) Banik, A.; Bandyopadhyay, T. K.; Biswal, S. K. Computational Fluid Dynamics (CFD) Simulation of Cross-Flow Mode Operation of Membrane for Downstream Processing,. *Recent Pat. Biotechnol.* **2019**, *13* (1), 57−68.

(26) Bandyopadhyay, T. K.; Das, S. K. Non-Newtonian and Gas-Non-Newtonian Liquid Flow through Elbows - CFD Analysis,. *J. Appl. Fluid Mech.* **2013**, *6* (1), 131−141.

(27) Mukherjee, H.; Brill, J.; Beggs, H. Experimental study of oil-water flow in inclined pipes. *J. Energy Resour. Technol.* **1981**, *103*, 56−66.

(28) Abduvayt, P.; et al. *Analysis of Oil−Water Flow Tests in Horizontal, Hilly-Terrain and Vertical Pipes*; SPE Annual Technical Conference and Exhibition, 2004.

(29) Soleimani, A. *Phase Distribution and Associated Phenomena in Oil−Water Flows in Horizontal Tubes*; Imperial College London (University of London), 1999.

(30) Kumara, W.; Halvorsen, B.; Melaaen, M. C. Pressure drop, flow pattern and local water volume fraction measurements of oil-water flow in pipes. *Meas. Sci. Technol.* **2009**, *20* (11), 114004.

(31) Alkaya, B.; Jayawardena, S.; Brill, J. Oil-water flow patterns in slightly inclined pipes. *Proceedings 2000 ETCE/OMAE Joint Conference, Petroleum Production Symposium*; American Society of Mechanical Engineers, 2000.

(32) Rodriguez, O.; Oliemans, R. Experimental study on oil-water flow in horizontal and slightly inclined pipes. *Int. J. Multiphase Flow* **2006**, *32* (3), 323−343.

(33) Banik, A.; Biswal, S. K.; Bandyopadhyay, T. K. Predicting the Optimum Operating Parameters and Hydrodynamic Behavior of Rectangular Sheet Membrane Using Response Surface Methodology Coupled with Computational Fluid Dynamics,. *Chem. Pap.* **2020**, *74*, 2977−2990.

(34) Moriasi, D. N.; Arnold, J. G.; Van Liew, M. W.; Bingner, R. L.; Harmel, R. D.; Veith, T. L. Model Evaluation Guidelines for Systematic Quantification of Accuracy in Watershed Simulations,. *Trans. ASABE* **2007**, *50* (3), 885−900.

(35) Kim, W.; Yoon, M.; Lee, M.; Park, S. CFD Analysis of Cavitation in a Crude Oil Pipeline to an Oil Tanker. *Comput.-Aided Chem. Eng.* **2012**, *31*, 580−584.

https://doi.org/10.1021/acsomega.3c05290
ACS Omega 2024, 9, 11181−11193